3D Unsteady Computations of Flapping Flight in Insects and Fish

R. Ramamurti and W.C. Sandberg
Laboratory for Computational Physics and Fluid Dynamics

Introduction: The flight of insects and birds and the swimming of fish have been sources of continuous fascination throughout the ages. Observation and controlled experimentation have historically been the main sources of information on performance. The mathematical description of the performance of flying creatures has been limited, due to the previously insurmountable difficulties associated with describing flapping wings with changing shape. Typical analytical descriptions are generally for steady flight only. Recent computational technology developments have enabled three-dimensional unsteady computations[1,2] to be successfully completed for flapping wings and deforming shapes. 3D unsteady computations, coupled with appropriate experiments, can now provide a more complete view of the fluid dynamics underlying the remarkable aerodynamic and hydrodynamic feats observed in insects, birds, and fish. If we seek to attain that level of performance in our designed vehicles, we still have much to learn. This paper briefly summarizes some attempts we have made at the Naval Research Laboratory (NRL) to gain insights into the unsteady aerodynamic performance of flying insects and swimming fish, and to incorporate that understanding into the design of unmanned underwater vehicles and unmanned air vehicles.

Underwater Flight: Our choice for a computational investigation of fin swimming was the bird wrasse (*Gomphosus varius*), shown in Fig. 4. This fish is reported to have excellent low-speed maneuverability and good high-speed propulsion—characteristics we are very interested in having in our vehicles. These fishes have been observed to fly underwater by flapping their pectoral fins with a motion that resembles the wing kinematics of certain flying insects. 3D unsteady computations were carried out for the wrasse with its pectoral fins executing the shape deformation time-history obtained from the measured fin kinematics. Figure 5 shows an instantaneous pressure distribution and the time history of lift and thrust production throughout several stroke cycles. An important objective, as we study the flow field evolution about the flapping fin and attempt to gain insights into the force production mechanism underlying the impressive dynamic performance of these living creatures, is to understand how variation of major design parameters changes the force production dynamics. For example, how important is the precise deformation time history of the fin for acceptable force production? Since the underwater vehicle design community has an aversion to deformable materials we need to understand what performance is sacrificed if we significantly alter the ability of the fin to deform. Our computations show that substantial penalty is incurred if we restrict the deformation of the fin. Detailed discussion of these results can be found in Ref. 3.

Maneuvering Insects: In addition to underwater vehicles we are also interested in the development of small unmanned air vehicles, referred to as Micro Air Vehicles (MAVs). We chose to pursue the fruit fly, *Drosophila*, for computational investigations since detailed wing kinematics and corresponding force data were available. The lift, thrust, and drag time histories and wing flow field evolution were computed about a single wing executing specified kinematics. The results of these computations were compared with experimental data and were extremely good. Since we must not be content with only good hovering or straight-ahead flight, we also considered the vehicle's ability to avoid obstacles. The motion of the fruit fly *Drosophila* involves several successive sharp turns called *saccades*. Since detailed kinematics and force measurements also exist for the *Drosophila* undergoing these turning maneuvers, we computed the flow over the wing and the body during the maneuver for the complete two-wing and body, with specified kinematics. The differences in the kinematics between the right and left wings show that subtle change in stroke and deviation angles can result in the yaw moment required for the turning maneuver. The origin of the yaw moment is investigated by computing the center of pressures on each wing and the individual moment arms. This investigation[4] leads to the conclusion that it is the forward force and a component of the lift force that combine to produce the turning moment while the side force alone produces the restoring torque during the maneuver. The vorticity shed from the wing's leading edge and the tips (Fig. 6) show a loop-like structure that during stroke reversals pinches off into Λ-like structures that have not been previously observed in the wakes of flapping fliers.

Unmanned Vehicles: We have computed the unsteady dynamics about the rigid wing of a flapping fruit fly and about the deforming pectoral fin of a swimming bird wrasse. The unsteady computations have been compared with experimental data and found to be in excellent agreement. Based on these computations and realizing that birds and insects do not have substantial fixed lifting surfaces unrelated to propulsion and control, the Tactical Electronic Warfare Division

Report Documentation Page

Form Approved
OMB No. 0704-0188

1. REPORT DATE **2007**	2. REPORT TYPE	3. DATES COVERED **00-00-2007 to 00-00-2007**

4. TITLE AND SUBTITLE **3D Unsteady Computations of Flapping Flight in Insects and Fish**	5a. CONTRACT NUMBER 5b. GRANT NUMBER 5c. PROGRAM ELEMENT NUMBER
6. AUTHOR(S)	5d. PROJECT NUMBER 5e. TASK NUMBER 5f. WORK UNIT NUMBER
7. PERFORMING ORGANIZATION NAME(S) AND ADDRESS(ES) **Naval Research Laboratory,4555 Overlook Avenue SW,Washington,DC,20375**	8. PERFORMING ORGANIZATION REPORT NUMBER
9. SPONSORING/MONITORING AGENCY NAME(S) AND ADDRESS(ES)	10. SPONSOR/MONITOR’S ACRONYM(S) 11. SPONSOR/MONITOR’S REPORT NUMBER(S)

12. DISTRIBUTION/AVAILABILITY STATEMENT
Approved for public release; distribution unlimited

13. SUPPLEMENTARY NOTES

14. ABSTRACT

15. SUBJECT TERMS

16. SECURITY CLASSIFICATION OF:			17. LIMITATION OF ABSTRACT	18. NUMBER OF PAGES	19a. NAME OF RESPONSIBLE PERSON
a. REPORT **unclassified**	b. ABSTRACT **unclassified**	c. THIS PAGE **unclassified**	**Same as Report (SAR)**	**6**	

Standard Form 298 (Rev. 8-98)
Prescribed by ANSI Std Z39-18

FIGURE 4
Bird wrasse in natural environment.

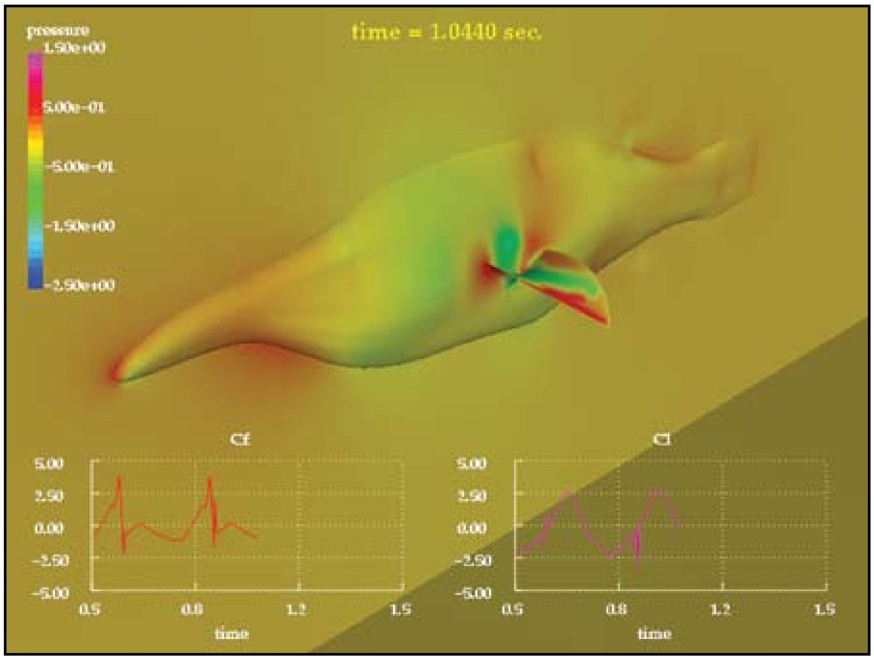

FIGURE 5
Surface pressure distribution, thrust, and lift time histories for a swimming bird wrasse.

at NRL developed a vehicle, the Biplane Insectioid Travel Engine (BITE), that has no fixed lifting surface but uses two tandem sets of clapping pairs of reversing camber wings. The reversing camber flapping wing has proven to be a versatile mechanism for producing thrust/lift without copying the insects' flying configurations directly. Computational studies (Fig. 7) show that the BITE-wing configuration is capable of producing sufficient thrust and lift using four reversing-camber tandem clapping wings. This configuration is amenable to some form of vortex capture mechanism, as seen in fruit flies and other two-winged insects. An underwater counterpart with flapping deforming fins is also being developed at NRL in collaboration with Dr. B. Ratna of the NRL Center for Bio/Molecular Science and Engineering.

Acknowledgments: This work was supported by the Office of Naval Research through the NRL Undersea Warfare Focus Area Swimming Vehicles Project with Dr. Edward Franchi as the Technical Monitor, and the NRL Tactical Electronic Warfare Division Micro Air Vehicles Program with Dr. Jim Kellogg as the Technical Monitor. The authors would like to thank Prof. Rainald Löhner of George Mason University for his support. The computations were supported in part by a grant of HPC time from the DoD HPC centers ARL MSRC SGI-O2K and NRL SGI-O2K.

[Sponsored by ONR]

References

[1] R. Ramamurti and W.C. Sandberg, "A 3-D Computational Study of Aerodynamic Mechanisms of Insect Flight," *J. Exp. Biol.* **205**, 1507-1518 (2002).

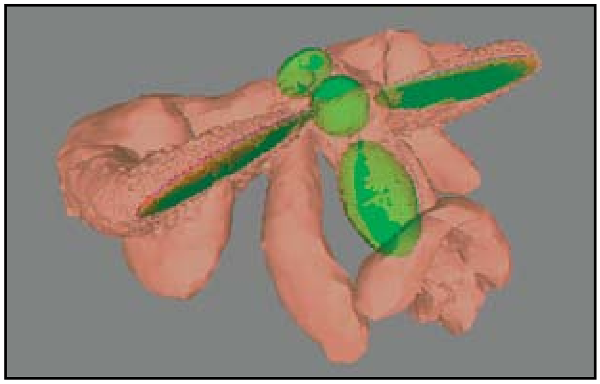

FIGURE 6
Contours of iso vorticity shed from the wings of *Drosophila* during maneuver.

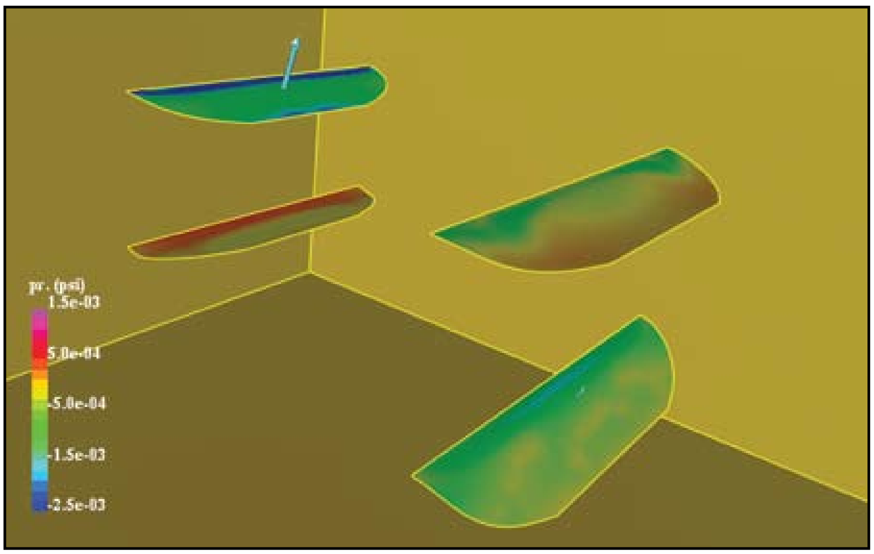

FIGURE 7
Surface pressure on the wings of the BITE vehicle at maximum lift.

[2] R. Ramamurti, W.C. Sandberg, R. Löhner, J.A. Walker, and M.W. Westneat, "Fluid Dynamics of Flapping Aquatic Flight in the Bird Wrasse: Three-dimensional Unsteady Computations with Fin Deformation," *J. Exp. Biol.* **205**, 2997-3008 (2002).
[3] R. Ramamurti and W.C. Sandberg, "The Influence of Fin Rigidity on the Force Production in the Bird-Wrasse: A Computational Study," NRL Memorandum Report 6410--04-8840, November 2004.
[4] R. Ramamurti and W.C. Sandberg, "A Computational Investigation of the Three-dimensional Unsteady Aerodynamics of *Drosophila* Hovering and Maneuvering," *J. Exp. Biol.* **210**, 881-896 (2007).

Highly Efficient Surface Enhanced Raman Scattering (SERS) Nanowire/Ag Composites

S.M. Prokes, O.J. Glembocki, and R.W. Rendell
Electronics Science and Technology Division

Introduction: Optically based sensing provides advantages over electronic sensing because optical spectra can uniquely fingerprint a chemical compound, significantly reducing false alarms and simplifying the detection process. In addition, light can easily be directed over long distances, enabling remote sensing. One of the most promising optical sensing techniques is surface enhanced Raman scattering (SERS). In Raman scattering (RS) of light from a chemical of interest, the vibrational modes in the chemical red-shift the frequency of the scattered light, producing a spectrum characteristic of that molecule. Ordinary Raman scattering cross-sections are very small, resulting in low sensitivity (1E-8 of the intensity of the exciting laser); this is not a problem for most solids and liquids, because of the large numbers of molecules or atoms exposed to the laser light, but in the case of trace amounts of molecules in gases or liquids, detection through ordinary Raman scattering is virtually impossible. However, SERS enhances the Raman signal by many orders of magnitude by the use of a substrate of metal nanoparticles.[1] The SERS enhancement of molecules adsorbed on the roughened metal surface is caused by local electromagnetic fields that are created by the laser excitation of surface plasmons at the metal surface. Even larger SERS effects can be produced by local "hot spots" in the electric fields, produced by interactions of localized plasmons on adjacent or neighboring nanoparticles.[2] Although the SERS effect has been recognized for a long time, a full understanding of the phenomenon has not yet been achieved. This lack of understanding limits its application potential, as it is difficult to produce highly sensitive, inexpensive, and repeatable SERS substrates. To address these issues, we have developed a new SERS substrate material consisting of dielectric/Ag metal shell nanowires that exhibit high SERS sensitivity due to their plasmonic coupling. These nanowires are sensitive at low concentrations, quite repeatable, and inexpensive to produce.

Technical Approach: The growth of the Ga_2O_3 nanowires was performed by vapor-liquid-solid (VLS) growth in a tube furnace, using Si(100) and Si(111) substrates and a 20 nm Au film.[3] Ga (99.995% purity) and oxygen were used as the source materials and the growth was performed at 900 °C at a vacuum of 10^{-2} Torr. The Ag shell coating was deposited via e-beam evaporation under high vacuum conditions. The SERS sensitivity of the nanowire substrates has been determined using Rhodamine 6G/methanol and DNT/methanol dilutions. The Ga_2O_3/Ag nanowire composite substrates are shown in Fig. 8(a). As can be seen, they consist of a dense random 3D network of crossed wires. A comparison of the SERS signal from 0.2 picograms of Rh6G for the nanowire composite substrates and a commercially available SERS substrate (Klarite) from Mesophotonics Ltd is shown in Fig. 8(b). As shown, no SERS signal is evident in the case of the commercial Mesophotonics sample, while a strong SERS signal is clearly seen for the nanowire composites. From these results, the nanowire/Ag composite substrate can repeatably exhibit an enhancement which is roughly two orders of magnitude higher than the commercially available SERS substrate.

The SERS of Rh6G, using the nanowire/metal random 3D arrays, has also been measured to be several orders of magnitude more sensitive than other SERS substrates, such as Ag nanosphere arrays produced by the Tollen's reaction, SiO_2/Ag nanosphere composites, polystyrene/Ag nanosphere composites, and roughened metal surfaces. In addition, these wires have exhibited sensitivity to DNT—which has a very low vapor pressure and is thus difficult to detect—better than picograms (shown in Fig. 9); this is the first reported SERS measurement of DNT using Ag metal nanostructures.

Furthermore, these nanowire composites can easily be removed from the substrate by sonication in an ethanol solution, and show an enhanced SERS signal even when deposited in a significantly dilute form. This opens up the possibility of covert tagging and tracking applications.

The most intriguing result from this work indicates that randomly crossed wires increase the SERS enhancement in the vicinity of the regions where wires cross, as shown in Fig. 10(a). The effect on the plasmon resonance by wire crossings can be modeled using a finite element Comsol[4] simulation of the electric field near two 45-nm-diameter Ag crossed wires in response to light polarized in the x-direction (Fig. 10(a)). The crossing of the nanowires leads to coupled plasmon behavior that spatially extends the sensitivity of the nanowires to encompass the regions between the wires and significantly beyond the wires. This would not only enhance the SERS effect due to the strong coupling, but also allow more molecules to enter this high electric field region, thereby enhancing the SERS sensitivity. In the case of two Ag nanospheres of the same diameter, the enhancement spatial extent is significantly smaller, as shown in Fig. 10(b). In addition, the nanosphere geometries require a very specific spacing in order to maximize the enhancement due to coupling, which is not the case in crossed wires, since an optimal spacing is always present for every crossing angle due to the wire geometry. As a simple rule of thumb, the sensitivity regions for the wires are within a sphere whose diameter is the length of the longest wire, which is a

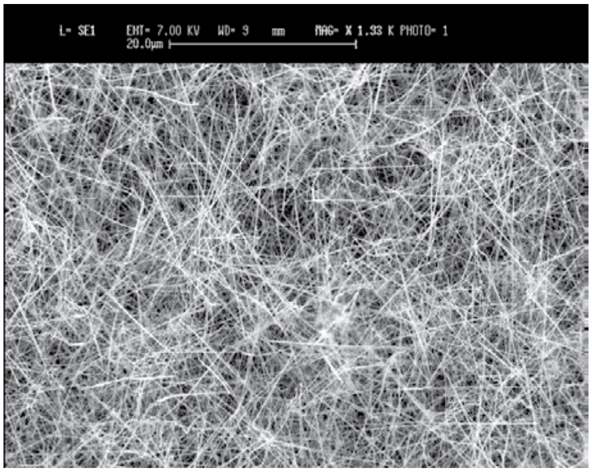

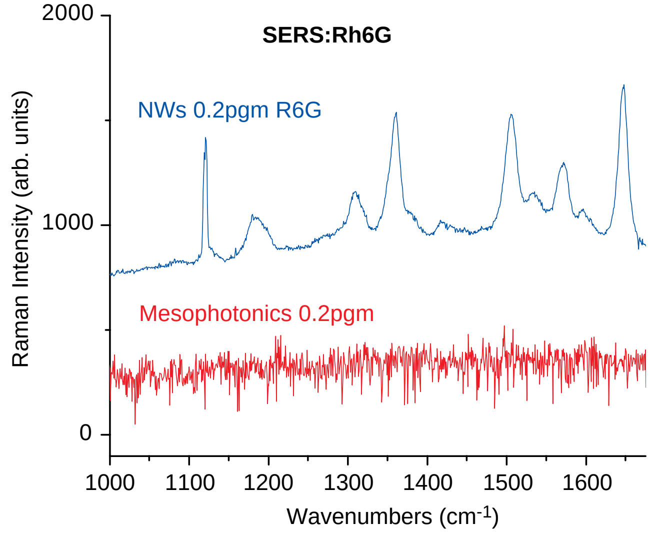

(a)

(b)

FIGURE 8
(a) Ga_2O_3 core/Ag shell nanowire composite and (b) comparison of SERS signal for Mesophotonics "Klarite" commercial substrate and Ga_2O_3/Ag nanowires.

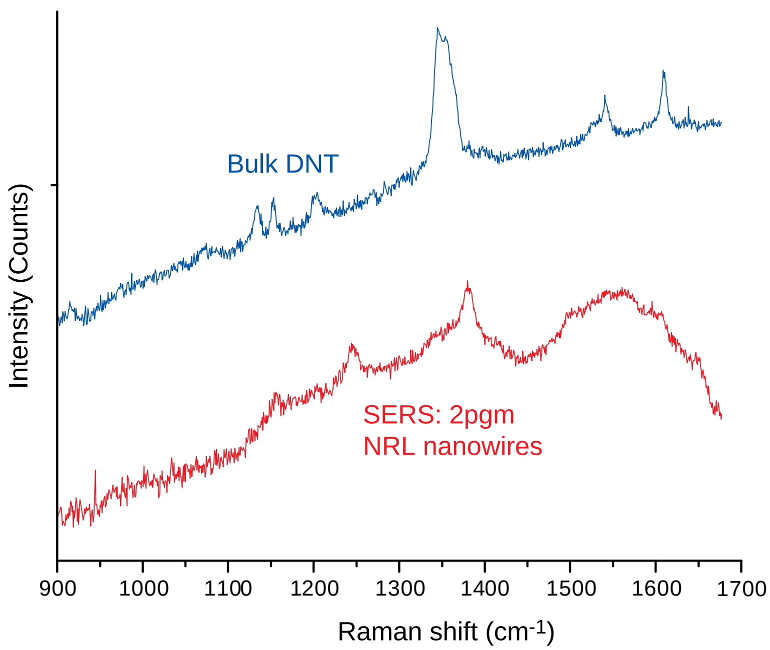

FIGURE 9
Raman spectrum of bulk DNT and a SERS spectrum of 2 picograms of DNT obtained from the dielectric/Ag nanowires.

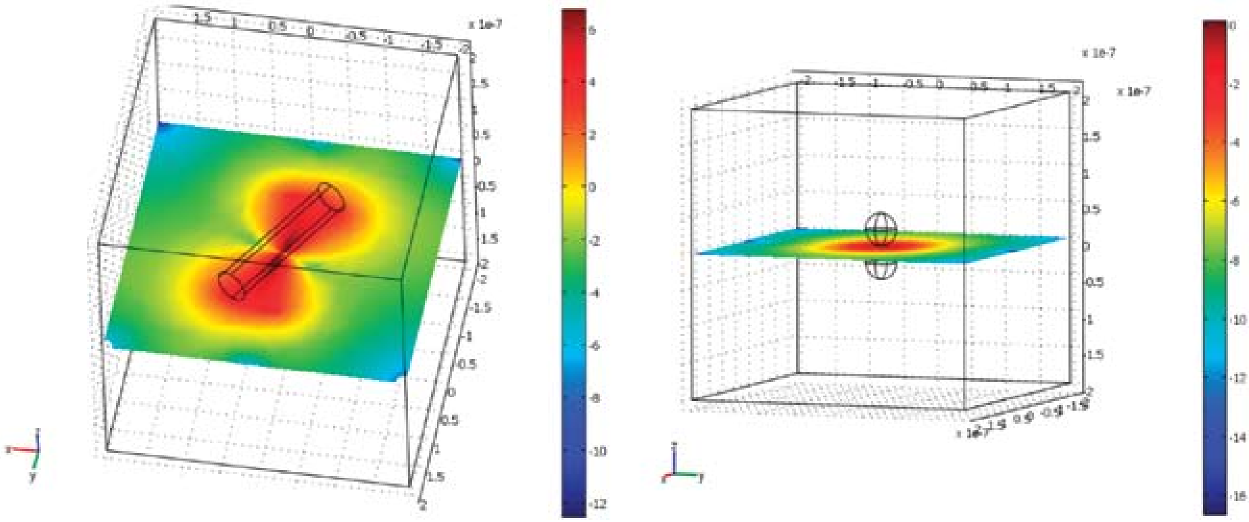

(a)

(b)

FIGURE 10
Comsol electric field simulations for (a) Ag crossed nanowires and (b) same diameter Ag nanospheres. Note the much larger area of enhancement in the case of the nanowires.

significant improvement over nanosphere-type SERS substrates.

Conclusion: Randomly oriented Ga_2O_3/Ag nanowire networks have been formed and we have shown that these substrates result in highly sensitive SERS signals using Rhodamine 6G as well as DNT. It is suggested that this SERS sensitivity is due to the formation of a large number of "hot spots" (enhanced electric fields due to plasmon coupling) when arranged in a random crossing geometry. Finite element calculations show significantly enhanced electric fields in the regions of the wire crossing, as well as surrounding the crossed wires, in support of the experimental results.

Due to these highly efficient hot spot regions formed by the crossing of the nanowires, we have also demonstrated that large SERS enhancements are possible even when the density of the nanowire network is significantly reduced. Since these wires can be deposited at low concentrations on any substrate and any size area, they have potential in applications such as large area sensor arrays, covert tagging, and remote sensing.

[Sponsored by ONR]

References

[1] M. Fleischman, P.J. Hendra, and A.J. McQuillen, *Chem. Phys. Lett.* **26**, 163 (1974); D.L. Jeanmaire and R.P. van Duyne, *J. Electroanal. Chem.* **84**, 1 (1977).
[2] J.B Jackson, S.L. Westcott, L.R. Hirsch, J.L. Wet, and N.J. Halas, *Appl. Phys. Lett.* **82**, 257 (2003).
[3] S.M. Prokes, W.E. Carlos, and O.J. Glembocki, *Proc. of SPIE* **6008**, 60080C-1 (2005).
[4] Comsol Multiphysics, Comsol, Inc., www.comsol.com.